Rev.Adv.Mater.Sci. 18(2008) 549-552

INFLUENCE OF Mn CONTENT ON THE MICROSTRUCTURE AND HYPERFINE INTERACTION PARAMETERS OF AMORPHOUS AND NANOCRYSTALLINE HITPERM-TYPE FeCoMnNbB ALLOYS

H. Benaini[1], J.S. Blázquez[1], C.F. Conde[1], A. Conde[1] and P. Ochin[2]

[1]Departamento de Física de la Materia Condensada. ICMSE-CSIC. Universidad de Sevilla. P.O. Box 1065. 41080 Sevilla, Spain
[2]ICMPE Institut de Chimie et des Materiaux Paris Est. CNRS-Universite Paris XII (UMR 7182). 2-8 rue Henri Dunant F-94320. Thiais, France

Received: March 29, 2008

Abstract. Effects of Mn addition on the devitrification kinetics, microstructure and hyperfine interaction parameters of FeCoMnNbB alloys were investigated. As-cast and nanocrystalline samples were studied by different experimental techniques and results were correlated. Mn alloying provoked a significant lowering of the Curie temperature of the amorphous phase. No big changes were observed in the microstructure of the nanocrystalline alloys with the Mn addition.

1. INTRODUCTION

Partial substitution of Co for Fe in Fe-based nanocrystalline alloys (α-Fe nanocrystals embedded in an amorphous matrix) yielded the development of HITPERM alloys [1], which extended the good soft magnetic properties of these systems up to higher temperatures due to the increase of the Curie temperature of the amorphous matrix, T_C^{am}. A higher T_C^{am} increases the maximum temperature at which the magnetic coupling between nanocrystals effectively average out the magnetocrystalline anisotropy [2]. Compositional tailoring of HITPERM alloys by addition of other elements (Mn, Ge) to optimize their physical properties has been carried out in some recent works [3,4]. Previous work on Mn effect on FINEMET alloys can be found in the literature [5]. In this work, the effect of Mn addition on the $Fe_{60-X}Co_{18}Mn_XNb_6B_{16}$ (X = 2,4) alloy series is studied for amorphous and nanocrystalline samples.

2. EXPERIMENTAL

Amorphous ribbons (30 μm thick and 10 mm wide) were prepared by planar flow casting method. Differential scanning calorimetry (DSC), thermomagnetic gravimetry (TMG), X-ray diffraction (XRD), transmission electron microscopy (TEM) and ^{57}Fe Mössbauer spectroscopy (MS) were used in this study. The MS spectra were fitted with NORMOS program [6].

3. RESULTS AND DISCUSSION

Fig. 1 shows the nanocrystalline microstructure developed during primary crystallization. The analysis of XRD patterns shows no significant differences between the two studied alloys: amorphous plus α-Fe(Co,Mn) phase with a grain size ~12 nm and crystalline volume fraction ~60%. TEM images show similar microstructures of nanocrystals with irregular shape, ~15 nm in size, embedded in a

Corresponding author: A. Conde, e-mail: conde@us.es

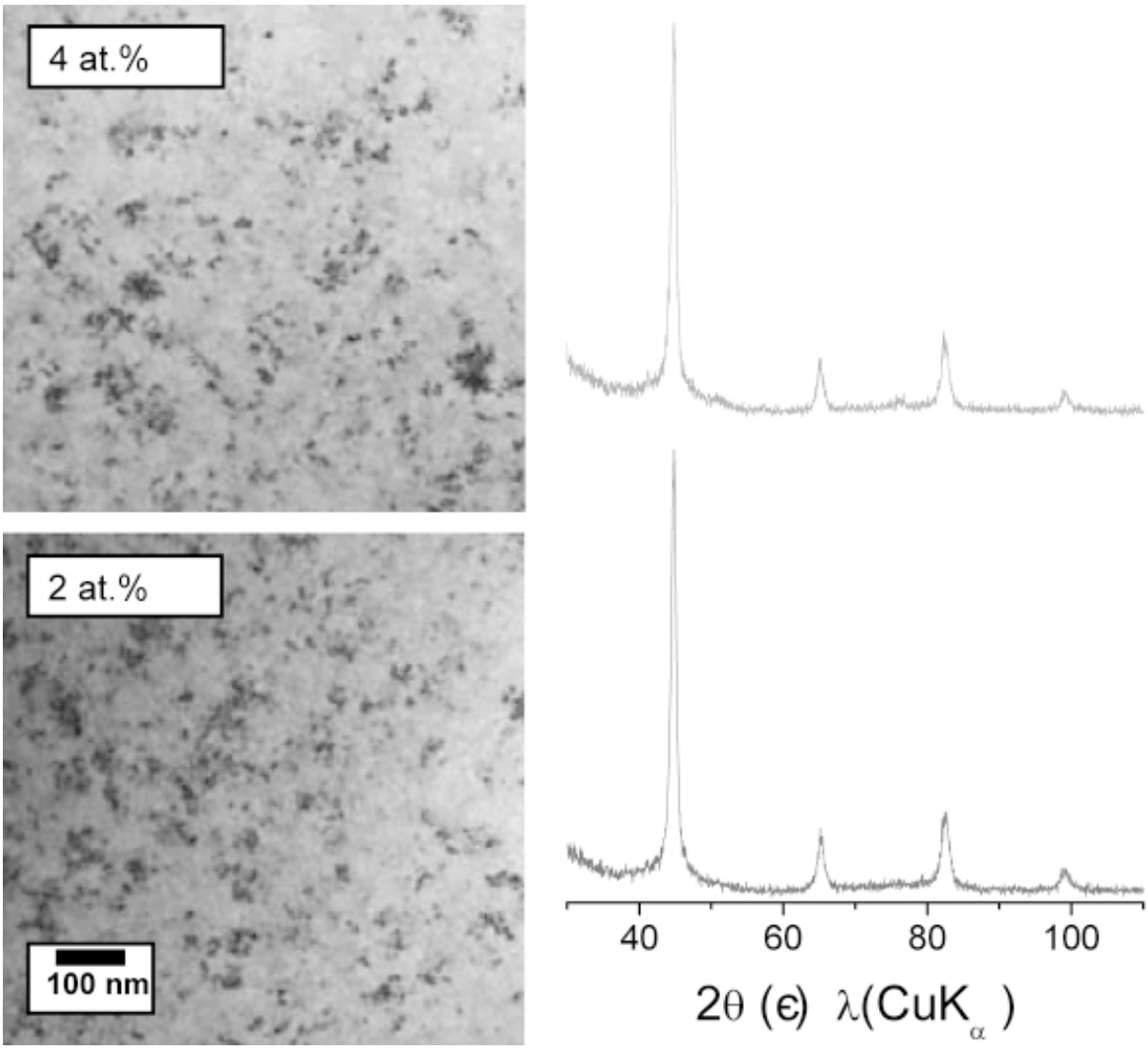

Fig. 1. Bright field TEM images and XRD patterns of nanocrystalline samples (heated up to 935K).

Table 1. Kinetic parameters: *n* Avrami exponent (at 773K), *Q* activation energy from the thermal dependence of induction time.

Mn (at.%)	*n* (initial)	*n* (final)	*Q* (eV)
2	0.91	0.28	3.8 ± 0.3
4	0.98	0.35	4.4 ± 0.3

residual amorphous matrix, in agreement with XRD results. The onset temperatures of the DSC exothermic peak, 780 and 787K for 2 and 4 at.% of Mn, respectively, are higher than that of the Mn free alloy (761K) [7]. The second DSC exothermic peak completes crystallization with the formation of boride phases. The kinetic parameters of the nanocrystallization process obtained from TMG isotherms are summarized in Table 1. The values describe a very slow kinetics characterized by an Avrami index ~1 and an activation energy ~4 eV, typical of nanocrystallization processes. TMG was also used to measure T_C^{am} (599 and 569K for 2 and 4 at.% of Mn, respectively). A strong reduction of T_C^{am} was found as the Mn content increases and with respect to the Mn free alloy (647K) [7].

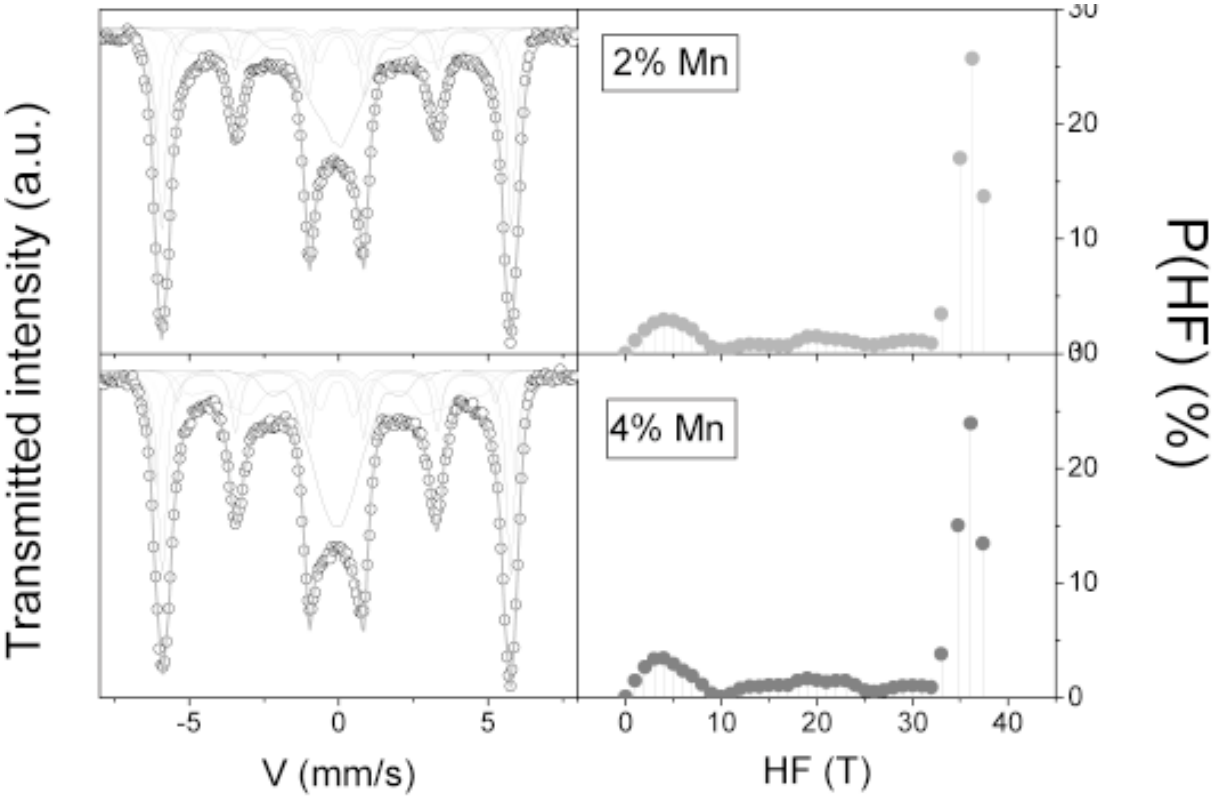

Fig. 2. Mössbauer spectra and probability distribution of hyperfine magnetic field contributions of the nanocrystalline samples.

MS spectra of as-cast samples (not presented here) show sextets with broadened and overlapped lines typical for amorphous alloys. They were fitted using a distribution of hyperfine magnetic fields (*HFD*). A bimodal *HFD* is observed with two overlapped peaks, centred at ~21 T and ~12 T, respectively. The former peak is ascribed to Fe without Nb as near neighbours and the latter one to Fe with Nb in their vicinity. For nanocrystalline samples (Fig. 2) the MS spectra were fitted using 4 values of hyperfine magnetic field, *HF*, (α-Fe,Co crystallites) and two *HFD* (amorphous phase and interface region). There is no difference between the average *HF* of the crystalline phase of both studied alloys (35.4 T), although the isomer shift, *IS*, for the alloy with 2 at.% Mn content is larger than for the alloy with 4 Mn at.% (*IS*=0.045 and *IS*=0.032 mm/s, respectively, relative to α-Fe foil at 300K). The large value of the average *HF* is due to the presence of Co inside the α-Fe crystals. Although the presence of Mn inside the crystals can not be unambiguously established, the effect of Mn on the global system is evidenced as a reduction of <*HF*> as the Mn content increases: for as-cast samples from 20.0 to 18.9 T and for nanocrystalline samples, from 26.8 to 25.7 T, for 2 and 4 at.% of Mn, respectively. For the nanocrystalline alloys studied, the fraction of Fe atoms located in crystalline sites was larger in the case of 2 at.% Mn alloy (60 %) than in the case of 4 at.% Mn (54 %). This difference could indicate that the Mn content in the α-Fe phase were larger for the 4 at.% Mn than for the 2 at.% Mn alloy, taking into account that from XRD the crystalline volume fraction is almost the same for both nanocrystalline alloys.

4. CONCLUSIONS

In conclusion, small Mn addition does not affect significantly the nanocrystalline microstructure of FeCoNbB alloys. The presence of Mn inside the nanocrystals can not be unambiguously asserted but its effect on the global system is clearly detected as a reduction of <*HF*> and T_C^{am}.

ACKNOWLEDGEMENTS

Work supported by the MEC of Spanish Government and EU FEDER (Project MAT2007-65227) and the Junta de Andalucìa (Project P06-FQM-01823). JSB is grateful to Junta de Andalucia for a research contract.

REFERENCES

[1] M.E. McHenry, M.A. Willard and D.E. Laughlin // *Progress in Mater. Sci*. **44** (1999) 291.
[2] A. Hernando, M. Vázquez, T. Kulik and C. Prados // *Phys. Rev. B* **51** (1995) 3581.
[3] C.F. Conde, A. Conde, P. Svec and P. Ochin // *Mat. Sci. Eng. A* **375-377** (2004) 718.
[4] J.S. Blázquez, S. Roth and A. Conde // *Acta Mater*. **53** (2005) 1241.
[5] C. Gómez-Polo, J.I. Pérez-Landazabal, V. Recarte, P. Mendoza-Zelis, Y.F. Li and M. Vázquez // *J. Magn. Magn. Mater*. **290-291** (2005) 1517.
[6] R. A. Brand, J. Lauer and D. M. Herlach // *J. Phys. F: Met. Phys*. **13** (1983) 675.
[7] J.S. Blázquez, C.F. Conde and A. Conde // *J. Non-Cryst. Solids* **287** (2001) 187.